VOLUME 35(1992), 2, 275–280
TRIBOLOGY TRANSACTIONS

Viscoelastic Effects in MIL-L-7808-Type Lubricant, Part II: Experimental Data Correlations©

N. H. FORSTER (Member, STLE) and J. B. SCHRAND
Aero Propulsion and Power Laboratory
Wright Patterson Air Force Base, Ohio 45433
and
P. K. GUPTA (Member, STLE)
PKG Inc.
Clifton Park, New York 12065

Viscoelastic behavior of the MIL-L-7808-type lubricant is modeled by correlating experimental traction data to rheological models based on lubricant viscosity, shear modulus and a critical or limiting shear stress. The two types of traction models used respectively employ a hyperbolic sine and inverse hyperbolic tangent function between the viscous shear strain rate and shear stress in the lubricant. While the viscosity-pressure-temperature relation is determined from viscosity measurements on a high-pressure viscometer, estimates of shear modulus and critical or limiting shear stress are derived by curve-fitting the model predictions to actual traction data obtained from a rolling-disk traction machine.

KEY WORDS

Traction, Viscosity, Film Thickness, Traction Modeling

INTRODUCTION

Lubricant behavior and the resulting traction or friction between mating surfaces of a rolling/sliding contact has been known to have a significant effect on the performance of mechanical components, such as bearings, gears, cams and cam followers, used in a wide range of rotating machinery systems. Under high speeds and heavy loads, the lubricant mechanics are too complex to be modeled by simple Newtonian behavior, and viscoelastic effects have been known to become more significant. Due to such complex mechanics of lubricant flow in a concentrated contact, it is generally very difficult to determine all the required fundamental properties of the lubricant by an independent bench test. An acceptable approach has been to carefully instrument a single contact, measure the traction force under the prescribed operating condition, and fit the model predictions to the measured data to estimate values of the appropriate rheological constants. Such an approach has been the basis for the present investigation which considers the viscoelastic behavior of the commonly used MIL-L-7808-type lubricant.

The current development effort is divided into three parts. In the first part (*1*), the analytical formulations for the traction models are developed. Part II, the present study, is devoted to the derivation of appropriate rheological constants of the lubricant. Finally, the effect of the fundamental lubricant behavior on the performance of a high-speed ball bearing shall be modeled in a future work, which will form Part III of this overall investigation (*2*).

It must be emphasized that lubricant rheology and traction have been a subject of considerable interest over the pat two decades. As already discussed in the first paper (*1*), the rather large amount of available literature considers a wide range of investigations dedicated to understanding the subtle mechanics of lubricant flow in a rolling/sliding contact. The present investigation implements the available models to the lubricant under consideration. It is expected that the correlations between model predictions and experimental observations, reported herein, shall be of some practical significance in the design of mechanical components.

Two sets of experiments are used to develop the constitutive constants of the lubricant. A high pressure viscometer is used to measure the viscosity-pressure-temperature relation, and a rolling-disk type apparatus is then used to measure traction in a concentrated contact. A brief review of these experimental setups is presented below before discussing the model correlations to the experimental data.

HIGH-PRESSURE VISCOMETER

A schematic diagram of the high-pressure viscometer used in the present investigation is shown in Fig. 1. The viscometer is based on the falling weight technique. The falling weight, or sinker, is a right circular cylinder with a coaxial hole for maximum fall velocity. The lubricant under test and the sinker are placed into the viscometer module, consisting of a non-magnetic stainless steel tube around which four coils are wrapped, one at the top to lift the sinker and

Presented at the 45th Annual Meeting in Denver, Colorado May 7–10, 1990 Final manuscript approved March 8, 1991

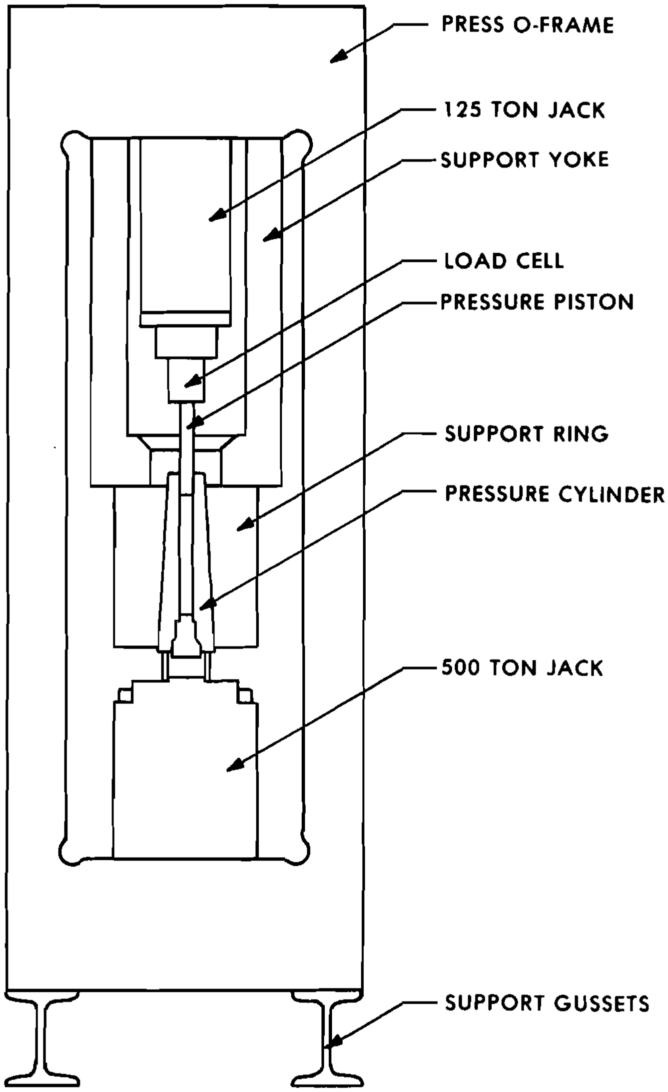

Fig. 1—Schematic diagram of the high-pressure viscometer.

three additional coils at the bottom that comprise a linear variable differential transformer (LVDT). The lubricant under test is separated from the pressure transmitting liquid by an O-ring seal in the top module, which is free to move up or down with changes in the density of the lubricant. The bottom of the module includes a socket with seven lug jacks which are plugged onto matching pins of closure at the bottom of the tapered cylinder. These electrical connections provide for the operation of the coil to lift the sinker, and for the operation of the LVDT to measure the position of the sinker. The sinker is constructed in three sections; the top and bottom are made from a highly permeable soft iron, and the middle is a nonmagnetic stainless steel. The inner and outer diameters of the sinker are 3.277 mm and 5.994 mm respectively, and the inner diameter of the tube is 6.350 mm. The viscosity of the lubricant is calculated by the method used by McLachlan (*3*):

$$\mu = \frac{C(\rho_s - \rho f)g}{V} \quad [1]$$

where ρ_s and ρf are, respectively, the densities of the sinker and the test fluid, g is the gravitational constant, V is the velocity of the sinker, and C is a constant at a particular temperature and pressure, determined experimentally by calibration. The calibration constant is corrected for dimensional changes due temperature and pressure by multiplying the calibration constant obtained at ambient temperature and pressure by the a correction factor, ψ_c, which is defined as:

$$\psi_c = \frac{\psi_p,T}{\psi_{amb}} \quad [2]$$

where ψ_p,T and ψ_{amb} are the values of a function ψ at any pressure p and temperature T, and at ambient conditions respectively. The function ψ is defined by Irving and Barlow (*4*) as:

$$\psi = \left[\frac{\ln(r_3/r_3) - (r_3^2 - r_2^2)^2}{(r_3^4 - r_2^4 + r_1^4)}\right](r_2^2 - r_1^2) \quad [3]$$

where r_1 is the radius of coaxial hole in the right cylinder of radius r_2, and r_3 is the radius of the tube in which the sinker, or the cylinder, falls with a constant velocity V.

The pressure-generating system consists of two 138 MPA air-operated pumps housed in a cabinet containing the valves and plumbing necessary to both advance and retract two hydraulic jacks, which are supported within an O-frame. The bottom 500-ton jack pushes the tapered cylinder into the support ring. The top 125-ton jack pushes the high pressure piston into the cylinder to generate lubricant pressures, in the test chamber, as high as 30 kbar.

Heat is provided by a set of band heaters clamped around the support cylinder and controlled by an iron-constantan thermocouple located between the band heaters and the support cylinder. The temperature of the lubricant is monitored by a chromel-alumel thermocouple located inside the pressure chamber.

TRACTION TESTER

The traction test machine consists of two rotating-disk specimens which are driven independently while a normal contact load is applied to establish a concentrated contact. The apparatus is illustrated in Fig. 2. The load is applied to the two rotating disk specimens through a pneumatic cylinder which supports the upper shaft assembly. Both rotating shafts are independently controlled by two 20-horsepower electric motors. Two magnetic speed pick-ups monitor the rotational speeds of the upper and lower shafts, and the traction force is measured by a rotating torque sensor mounted in line with the lower shaft. The lubricant temperature is measured by a thermocouple placed in the spray of an oil jet in close proximity to the rotating disk surfaces. A more comprehensive discussion of the basic test rig is presented by Smith et al. (*5*).

A desktop laboratory computer system is used to control the upper and lower shaft speeds, and is also used for data acquisition. The shaft speeds are controlled such that the average speed of the two disks is held constant, while respectively increasing and decreasing the speeds of the upper and lower disks to create slip. Such an approach permits

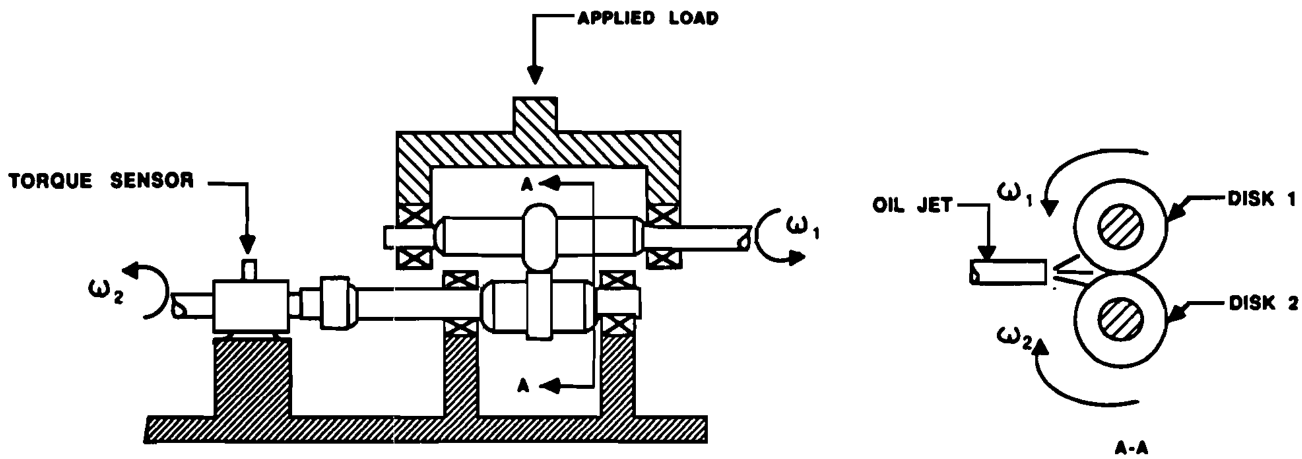

Fig. 2—Schematic of the traction test machine.

the generation of traction curves with variable slide-to-roll ratios while the rolling speed remains constant. The accuracy of the data is improved by eliminating a ramp function average rolling speed, which is an undesirable variable found in most traction test data. The applied load, torque, shaft speeds and oil inlet temperature are sampled at each speed increment during the test. Approximately 150 samples of the test variables are saved on a floppy diskette to produce a traction curve.

Table 1 summarizes the geometry of the test specimens used and the ellipticity ratio with each set of specimens. The ranges for rolling velocity, lubricant temperature and Hertzian contact pressure, over which the experimental data was obtained, are 20 to 80 M/S, 290 to 370° K, and 0.5 to 1.65 GPa respectively.

VISCOSITY DATA CORRELATIONS

As discussed in the authors' companion paper (*1*), the two most common types of viscosity-pressure-temperature relations are used to correlate the experimental viscosity data.

The viscosity, μ (Pa.S), at pressure, P (Pa), and temperature, T (°K), for the two types of relations is written as:

$$\mu = \mu_o \exp\left\{\sum_{i=1}^{n_1}\alpha_i p^i + \sum_{j=1}^{n_2}\beta_j \Delta T^j + \sum_{k=1}^{n_3}\gamma_k \Delta T^k\right\} \quad [4]$$

where:

$$\Delta T = (T_0 - T) \text{ for the Type I model, and}$$

$$\Delta T = \left(\frac{1}{T} - \frac{1}{T_o}\right) \text{ for the Type II model.}$$

Also, μ_o is the reference viscosity at atmospheric pressure and reference temperature T_o, α_i are the pressure-viscosity coefficients, β_j are the temperature-viscosity-coefficients and γ_k are the pressure-temperature-viscosity coefficients.

A linear regression analysis of the experimental data is carried out to compute the various coefficients in the viscosity relations. After several trials, it is found that two terms ($n_1 = n_2 = n_3 = 2$) in the generalized regression equation are adequate to describe the variation seen in the experimental data. The various coefficients of the Type I and Type II relations are summarized in Table 2.

A graphical representation of the data, indicated by data points, along with the regression fit, indicated by solid lines, is presented in Fig. 3 for the Type II model. Results for the Type I relation are similar.

TRACTION DATA CORRELATIONS

Once again, as discussed in the first part of this paper (*1*), two types of constitutive equations are considered for

TABLE 1—GEOMETRY OF TRACTION SPECIMENS

	DISK #1		DISK #2		
SET #	ROLLING RADIUS (mm)	CROWN RADIUS (mm)	ROLLING RADIUS (mm)	CROWN RADIUS (mm)	ELLIPTICITY RATIO
B	38.1	914.4	38.1	914.4	7.75
D	76.2	25.4	76.2	∞	1.31
E	38.1	257.1	38.1	257.1	3.50
G	38.1	9.525	38.1	−10.29	3.50
H	76.2	161.0	76.2	∞	2.59

TABLE 2—VISCOSITY COEFFICIENTS FOR THE MIL-L-7808 LUBRICANT

COEFFICIENT	TYPE I MODEL		TYPE II MODEL	
T_o	300	°K	300	°K
μ_o	0.032629	Pa.S	0.030391	Pa.S
α_1	$1.2788 \cdot 10^{-8}$	1/Pa	$1.2925 \cdot 10^{-8}$	1/Pa
α_2	$-2.4955 \cdot 10^{-18}$	$1/Pa^2$	$-2.4538 \cdot 10^{-18}$	$1/Pa^2$
β_1	$2.1530 \cdot 10^{-2}$	1/°K	$6.7295 \cdot 10^{2}$	°K
β_2	$6.4193 \cdot 10^{-6}$	$(1/°K)^2$	$-2.2642 \cdot 10^{6}$	(°K)
γ_1	$7.9284 \cdot 10^{-11}$	1/(Pa.°K)	$9.3937 \cdot 10^{-6}$	°K/Pa
γ_2	$2.2282 \cdot 10^{-22}$	$1/(Pa.\ °K)^2$	$2.9840 \cdot 10^{-12}$	$(°K/Pa)^2$

modeling the traction behavior. The general equation is written as:

$$\dot{s} = \frac{1}{G}\frac{\partial \tau}{\partial t} + \frac{\tau_o}{\mu} f\left(\frac{\tau}{\tau_o}\right) \quad [5]$$

where the three fundamental properties, e.g., G, τ_o, and μ, are the shear modulus, critical shear stress, and lubricant viscosity, respectively, and the functional relationship for the viscous terms in the two types of models is written as:

$$\text{Type I: } f\left(\frac{\tau}{\tau_o}\right) =$$

$$\sinh\left(\frac{\tau}{\tau_o}\right), \text{ the Johnson and Tevaarwerk (6) model}$$

$$\text{Type II: } f\left(\frac{\tau}{\tau_o}\right) =$$

$$\tanh^{-1}\left(\frac{\tau}{\tau_o}\right), \text{ the Bair and Winer (7) model}$$

A generalized regression analysis for the above viscoelastic models is numerically very cumbersome. However, in view of the above viscosity relations, obtained independently, the traction data correlations may be obtained by the following simplified procedure:

1. Based on the viscosity-pressure-temperature relation, compute an effective average viscosity under the operating conditions for a given traction curve.
2. From the experimental data, determine the values for traction slope at low slip rates, and the limiting traction coefficient at high slip rates. Use these values to estimate the shear modulus and the critical or limiting shear stress in the constitutive equation.
3. With the above preliminary values of shear modulus and critical shear stress, perform a regression analysis to minimize the squared deviation between the computed traction and corresponding experimental data. Such an analysis is carried out over the range of experimental operating conditions, and the variation of shear modulus and critical shear stress with pressure and temperature is derived.

The pressure and temperature dependence for the shear modulus, G, and critical shear modulus, τ_o, is assumed to be similar to the Type II viscosity relation:

$$G = \overline{G} \exp\left\{\alpha_G p + \beta_G\left(\frac{1}{T} - \frac{1}{T_o}\right)\right\} \quad [6]$$

$$\tau_o = \overline{\tau_o} \exp\left\{\alpha_\tau p + \beta_\tau\left(\frac{1}{T} - \frac{1}{T_o}\right)\right\} \quad [7]$$

The computed values for the various coefficients for the two types of traction models are summarized in Table 3. In terms of the physical interpretation of these correlations, it must be emphasized that use of the computed coefficients only provides a good overall correlation between the predicted and measured traction. The coefficients may not represent the true rheological constants of the lubricant.

Figures 4(a) and 4(b), show the correlation between predicted and measured traction with the Type I model for two sets of experiments carried out with the two greatly different values of the contact ellipticity ratios. Using Eqs. [6] and [7], the coefficients summarized in Table 3, and the viscosity relation summarized in Table 2, appropriate effective values of the rheological constants are calculated for the operating conditions corresponding to a given traction

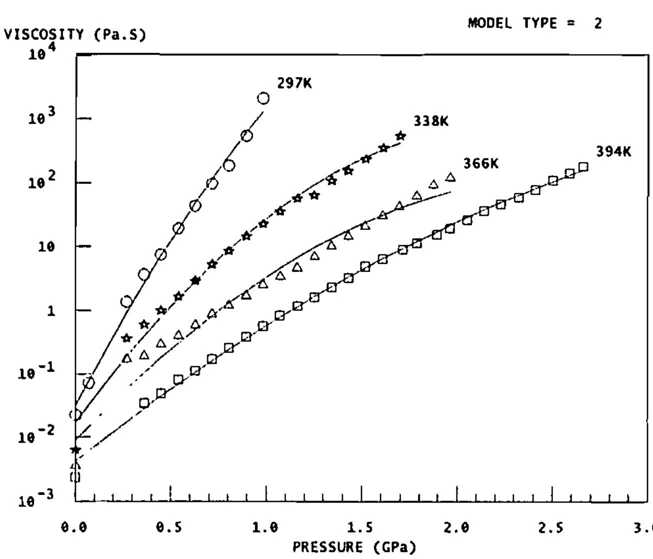

Fig. 3—MIL-L-7808 viscosity data fit to the Type II viscosity relation.

TABLE 3—SHEAR MODULUS AND CRITICAL SHEAR STRESS COEFFICIENTS FOR THE MIL-L-7808 LUBRICANT

COEFFICIENT	TYPE I MODEL		TYPE II MODEL	
T_o	300	°K	300	°K
$\overline{G}$	$8.00 \cdot 10^6$	Pa	$8.00 \cdot 10^6$	Pa
α_G	$3.35 \cdot 10^{-9}$	l/Pa	$3.35 \cdot 10^{-9}$	l/Pa
β_G	$3.00 \cdot 10^3$	°K	$3.00 \cdot 10^3$	°K
$\overline{\tau_o}$	$6.00 \cdot 10^5$	Pa	$1.50 \cdot 10^6$	Pa
α_τ	$1.25 \cdot 10^{-9}$	l/Pa	$2.45 \cdot 10^{-9}$	l/Pa
β_τ	$-8.00 \cdot 10^2$	°K	$1.20 \cdot 10^3$	°K}

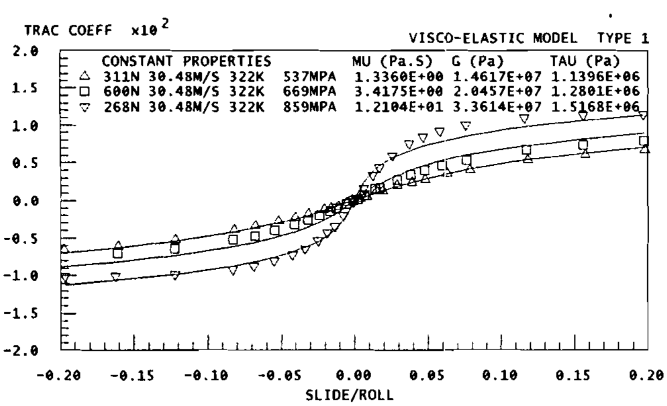

Fig. 4(a)—Typical correlations of the Type I traction model to experimental data with an ellipticity ratio of 7.75.

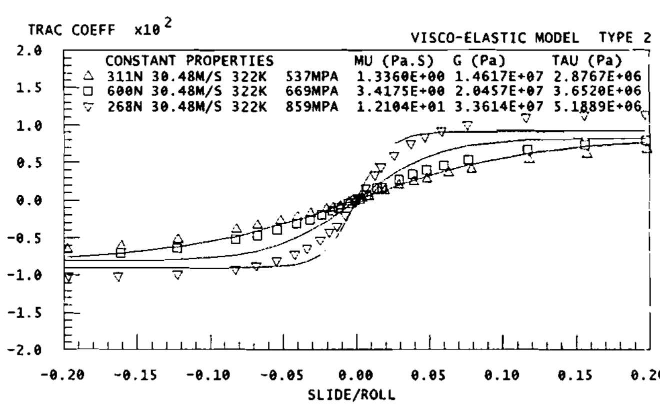

Fig. 5(a)—Typical correlations of the Type II traction model to experimental data with an ellipticity ratio of 7.75.

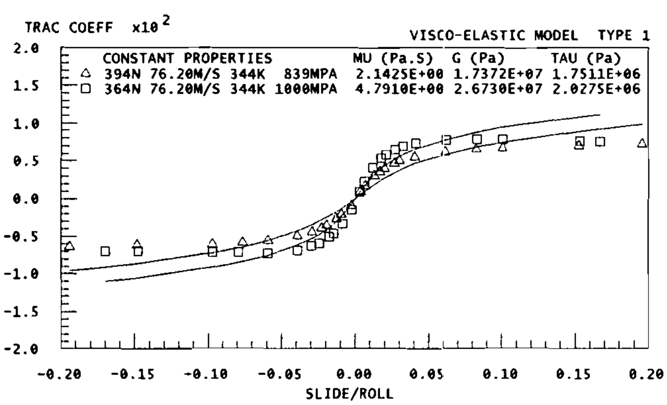

Fig. 4(b)—Typical correlations of the Type I traction model to experimental data with an ellipticity ratio of 2.59.

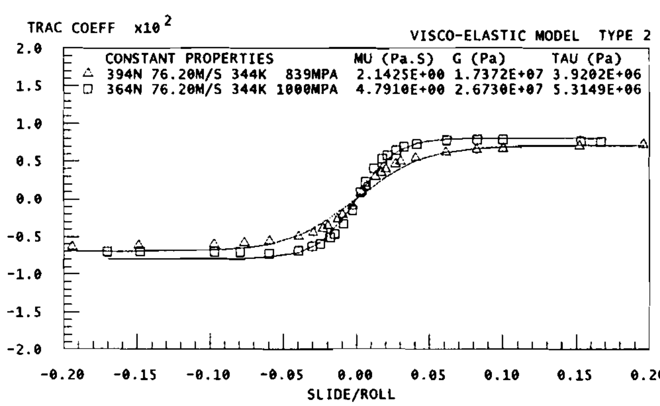

Fig. 5(b)—typical correlations of the Type II traction model to experimental data with an ellipticity ratio of 2.59.

curve. These values are then held constant within the contact ellipse to compute traction. Appropriate effective values of the rheological constants, as derived from the basic coefficients listed in Table 3, are summarized in the legend included in Figs. 4(a) and 4(b).

Correlations to the Type II model are shown in Figs. 5(a) and 5(b), for the two data sets used in Figs. 4(a) and 4(b) for the Type I model correlation. A comparison of these figures reveals that both models fit the data equally well.

While comparing the coefficients of the two models, it is seen that while the shear modulus values are identical, the critical shear stress parameter is somewhat higher for the Type II model in comparison to that of the Type I model. This difference is explained in terms of the physical definition of τ_o in the two models. It may be recalled from the earlier paper (*1*), that τ_o in the Type I model is a critical shear stress beyond which the viscous behavior becomes significant, while in the Type II model, it is simply a limiting shear stress which the lubricant can withstand. Such a definition also explains a slight slope in traction at high slip velocities with the Type I model, while it is relatively constant with the Type II model.

SUMMARY

Viscoelastic effects in the behavior of the MIL-L-7808-type lubricant are investigated by establishing significant correlations between model predictions and experimental observations. The models consist of three fundamental properties: viscosity, shear modulus and a critical or a limiting shear stress. While the effective viscosity is calculated from the viscosity-pressure-temperature relations developed from independent viscosity measurements, the experimental traction data is correlated to model predictions to estimate the average values of shear modulus and critical or limiting shear stress. The results are correlated over a range of pressures and temperatures and are summarized in terms of simple rheological equations which can be used for traction predictions.

ACKNOWLEDGMENTS

This work was sponsored by the Aero Propulsion and Power Laboratory at Wright-Patterson Air Force Base, contract number F33615-86-C-2696, under the Defense Small Business Innovation Research Program. Computational support was provided by the ASD Computer Center at Wright-Patterson Air Force Base.

REFERENCES

(*1*) Gupta, P. K., Cheng, H. S., Zhu, D., Forster, N. H. and Schrand, J. B., "Viscoelastic Effects in MIL-L-7808 Type Lubricant, Part I: Analytical Formulation," *Trib. Trans.*, **35**, 2, pp ——–—— (1992).

(*2*) Gupta, P. K., "Viscoelastic Effects in MIL-L-7808 Type Lubricant, Part III: High Speed Ball Bearing Response," *Trib. Trans.*, **35**, 2, pp ——–— (1992).

(*3*) McLachlan, R. J., "A New High-Pressure Viscometer for Viscosity Range 10 to 10^6 PaS," *Jour. of Phys. E: Scientific Inst.*, **9**, pp 391–394 (1976).

(*4*) Irving, J. B. and Barlow, A. J., "An Automatic High-Pressure Viscometer," *Jour. of Phys. E: Scientific Inst.*, **4**, pp 232–236 (1971).

(*5*) Smith, R. L., Walowit, J. A., Gupta, P. K. and McGrew, J. L., "Research in Elastohydrodynamic Lubrication of High Speed Rolling-Sliding Contacts," Air Force Technical Rpt. **AFAPL-TR-72-56** (1972).

(*6*) Johnson, K. L. and Tevaarwerk, J. L., "Shear Behavior of EHD Oil Films," *Proc. Roy. Soc. London*, **A356**, p 215 (1977).

(*7*) Bair, S. and Winer, W. O., "A Rheological Model of EHD Contacts based on Primary Laboratory Data," *ASME Jour. Lubr. Tech.*, **101**, 3, p 258 (1979).